The International Journal of
Robotics Research

Experiments in Balance with a 3D One-Legged Hopping Machine

Marc H. Raibert, H. Benjamin Brown, Jr and Michael Chepponis

Published by:

$SAGE

http://www.sagepublications.com

On behalf of:

Multimedia Archives

>> Version of Record - Jun 1, 1984

What is This?

Marc H. Raibert
H. Benjamin Brown, Jr.
Michael Chepponis

Department of Computer Science
and The Robotics Institute
Carnegie-Mellon University
Pittsburgh, Pennsylvania 15213

Experiments in Balance with a 3D One-Legged Hopping Machine

Abstract

In order to explore the balance in legged locomotion, we are studying systems that hop and run on one springy leg. Previous work has shown that relatively simple algorithms can achieve balance on one leg for the special case of a system that is constrained mechanically to operate in a plane (Raibert, in press; Raibert and Brown, in press). Here we generalize the approach to a three-dimensional (3D) one-legged machine that runs and balances on an open floor without physical support. We decompose control of the machine into three separate parts: one part that controls forward running velocity, one part that controls attitude of the body, and a third part that controls hopping height. Experiments with a physical 3D one-legged hopping machine showed that this control scheme, while simple to implement, is powerful enough to permit hopping in place, running at a desired rate, and travel along a simple path. These algorithms that control locomotion in 3D are direct generalizations of those in 2D, with surprisingly little additional complication.

1. Introduction

The ability to balance actively is a key ingredient in the mobility observed in natural legged systems and could be an important factor in human-made legged systems yet to be developed. Actively stabilized legged systems can move on a narrow base of support, permitting travel where obstacles are closely spaced or where the support path is narrow. Systems that balance need not be supported all the time and may therefore

---

use support points that are widely separated or erratically placed. This ability to place the feet on just those locations that provide good support increases the types of terrain a legged system can negotiate. Biological legged systems routinely operate with narrow base and intermittent support to traverse terrain too difficult for existing wheeled or tracked vehicles.

While the potential advantages of active stability and intermittent support may have been recognized for some time (Manter 1938; McGhee and Kuhner 1969; Frank 1970; Gubina 1972; Vukobratović 1973), progress in building legged systems that employ such principles has been retarded by the perceived difficulty of the task. As a result, much of the previous work on walking machines has taken a quasi-static approach, operating at low velocity with continuous and broad-based support (Frank 1968; Bessonov and Umnov 1973; McGhee and Buckett 1977; Hirose and Umetani 1980; Sutherland 1983). These devices have four or six legs, with at least three legs providing support at all times.

Our previous work has shown experimentally that it is possible to control a dynamic legged system that balances actively as it hops and runs (Raibert and Brown, 1984). However, the apparatus of those experiments was a planar device that was constrained mechanically to move with just three degrees of freedom. Useful locomotion takes place in 3D space, where motion with six degrees of freedom is possible. In this paper we present algorithms that control a legged system that balances as it hops and runs in 3D and experimental data that characterize the performance. These experiments show that, in the context of a hopping machine with a single springy leg, the control problem need not be difficult at all. A very simple set of algorithms is sufficient to control the machine as it hops in place, as it travels from point to point under velocity or position control, and as it responds to external mechanical disturbances. The control algorithms are direct generalizations of those used in 2D.

1.1. BACKGROUND

Previous work on balance began with Cannon's control of inverted pendulums that rode on a small powered truck (Higdon and Cannon 1963). His experiments included balance of a single pendulum; two pendulums, one atop the other; two pendulums side by side; and a long limber pendulum. They controlled the tipping moments by manipulating the point of support with state feedback. Hemami and his co-workers (Golliday and Hemami 1977; Hemami and Golliday 1977; Hemami and Farnsworth 1977; Ceranowicz 1979; Hemami 1980), Vukobratović and his co-workers (Vukobratović and Stepaneko 1973; Vukobratović and Okhotsimskii 1975), and others (Frank 1970; Bessonov and Umnov 1973; Beletskii and Kirsanova 1976) have studied the dynamic characteristics of a variety of multilink legged models that walk in simulation. In each case the models balance while maintaining continuous contact with the support surface.

Kato et al. (1981) have studied *quasi-dynamic* walking in the biped. In their experiments, a 40-kg biped with 10 hydraulically driven degrees of freedom temporarily destabilizes itself in order to transfer support from one large foot to the other. It uses a prerecorded sequence of motions to do this. Miura and Shimoyama (1980) have built a number of small electrically powered walking bipeds that balance using tabular control schemes. Their most advanced device, called the *stilt biped,* walks on two small feet while balancing in 3D. It has three actuated degrees of freedom that permit each leg to move fore and aft, to move sideways, and to lift slightly off the floor. It walks with a pronounced shuffling gait.

Systems with a ballistic phase have also been studied. Seifert (1967) explored the idea of using a large pogo stick for transportation on the moon, where low gravity would permit very long hops. He proposed using a moment-exchange gyroscope to reorient the body in flight. Matsuoka (1979) analyzed 2D hopping in humans with a one-legged model. He derived a time-optimal state-feedback controller that stabilized his model, assuming that the leg could be treated as massless, and that the stance period could be of very short duration. Matsuoka (1980) also implemented a physical planar one-legged hopping machine that operated in a very low-gravity environment by lying on a table inclined 10° from the horizontal.

Originally motivated by the conceptual similarity between a pogo stick and a leg, Raibert and his co-workers studied planar systems that hop and balance on one springy leg (Raibert, 1984; Raibert and Wimberly, 1984; Raibert and Brown, 1984). They found that for a system constrained to operate in 2D, control can be decomposed into three separate and very simple parts: one part to control forward running velocity, one to maintain the body in an erect posture, and one to regulate hopping height. These three parts of the control system were each synchronized to the ongoing activity of the hopping machine. This decomposition of the locomotion algorithm resulted in a particularly simple control design, and it provided a framework within which one can think about more complicated problems in locomotion.

In this paper, we extend these 2D results to a system that balances in 3D. The main finding is that very simple algorithms are adequate to control the locomotion of a one-legged machine that hops and runs in 3D. The 3D control algorithms are direct extensions of the 2D algorithms, relying on the same three-part decomposition. The sections that follow describe the physical hopping machine that was used for experiments, review the 2D control algorithms and describe their generalization to 3D, and present experimental data that illustrate the 3D system's ability to balance and run under a variety of conditions.

2. 3D Hopping Machine

The hopping machine shown in Figs. 1 and 2 was designed for experiments on balance in 3D. The main parts are a springy leg and a body, connected by a gimbal-type hip. Actuators control the orientation of the leg with respect to the body and the axial thrust delivered by the leg. Sensors provide state information from the hip, leg, and body to a control computer located nearby in the laboratory.

The body consists of a lightweight platform and roll cage, on which are mounted sensors, valves, actuators, and interface electronics. The ratio of moment of inertia of the body to that of the leg is about 6.5/1. This relatively high ratio ensures that movement of the

Fig. 1. Diagram of the 3D one-legged machine used for experiments. It has two primary parts: a body and a leg. The body is made of an aluminum frame, on which are mounted hip actuators, valves, gyroscopes, and computer interface electronics. The leg is a pneumatic cylinder with a padded foot at one end and a linear potentiometer at the other end. Two two-way pneumatic valves control the flow of compressed air to and from the lower end of the leg actuator. A pressure regulator and check valve control the pressure in the upper end of the leg actuator. The leg is springy because air trapped in the leg actuator compresses when the leg shortens. The leg is connected to the body by a gim-bal-type hip with two degrees of freedom. A pair of low-friction hydraulic actuators powered by pressure-control servo valves act between the leg and body to determine the hip angles. Sensors measure the length of the leg, the length and velocity of each hydraulic actuator, contact between the foot and the floor, pressures in the leg's air cylinder, and the pitch, roll and yaw angles of the body. Analog measurements are digitized on the machine and transmitted to the control computer over a parallel digital bus. An umbilical cable connects the machine to hydraulic, pneumatic, and electrical power supplies, and to the control computer, all of which are located nearby in the laboratory.

Fig. 2. Photograph of the 3D one-legged machine in midstride. The machine is running from left to right at about 1.8 m/s (3.9 mi/h).
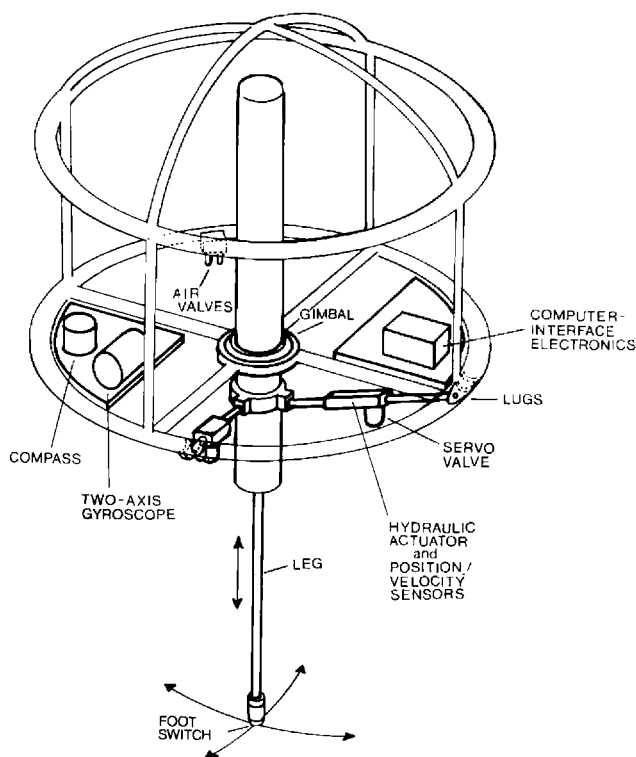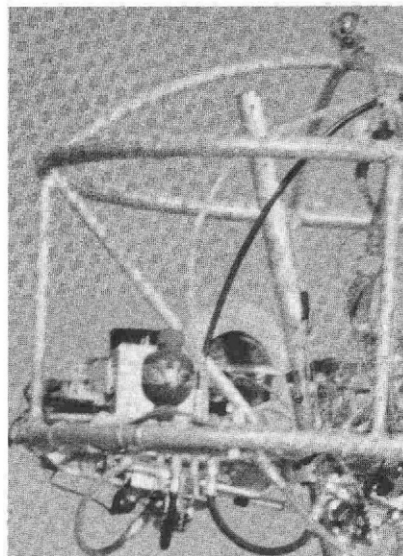
leg during flight does not severely disturb the attitude of the body. The center of mass of the body is located very close to the hip, so the only moments acting on the body are those generated by the hip actuators. A pair of free gyroscopes mounted on the body provide measurements of the roll, pitch, and yaw angles of the body with respect to fixed space. The roll cage protects the hopping machine when it falls over, and also provides convenient handles during experiments.

The leg is a double-acting air cylinder. The arrangement of pneumatic cylinder, pressure regulator, and check valve forms an air spring that absorbs energy when the leg shortens under external load and supplies energy when the leg lengthens. It is storage and recovery of energy in this air spring that transfers the kinetic energy from one hop to the next hop, thereby re-

Raibert, Brown, and Chepponis   **77**

ducing the cost of continuous hopping. The upper chamber of the pneumatic cylinder that forms the leg actuator is connected to a pressure regulator that maintains its minimum pressure. This regulator was set to values between 40 and 75 psi for the present set of experiments. A check valve permits the pressure to increase when the leg is compressed, without forcing air back through the system.

The hopping motion is produced by the flow of compressed air to and from the lower chamber of the leg actuator. A pair of two-way solenoid valves permits this chamber to be pressurized to 80 psi or exhausted. When it is pressurized it causes the piston to move upward and the leg to shorten, and when it is exhausted it causes the piston to move downward and the leg to lengthen. The timing of pressure and exhaust are chosen to excite the spring-mass oscillator formed by the leg and body. Peak-to-peak amplitude of body oscillation under ideal conditions varied between 0.02 and 0.5 m, with corresponding bouncing frequencies of about 3.0 to 1.5 per second. Over this range of bouncing frequencies the stance period is nearly constant, varying by only a few percent, as expected for a spring-mass system.

A rubber cushion is attached to the lower end of the leg-actuator rod to form a foot. The area of the foot that contacts the ground is only about 1 cm^2, providing a good approximation to a point support. The coefficient of friction between the foot and the floor in our laboratory is about 0.6. The foot has a built-in switch that tells the control computer when there is contact with the ground. The upper end of the actuator rod carries a wiper that forms the moving element of a linear potentiometer used to measure the length of the leg.

The leg and body are connected by a gimbal joint that forms a hip. A pair of linear hydraulic actuators controls the angles between the body and the leg. These hip actuators use only low-pressure seals and a leaky piston to provide very low static friction. Each hip actuator has a pressure-control servo valve, a linear potentiometer, and a linear tachometer. The control computer servos the length of these actuators, and therefore the angles between leg and body, with a pair of linear servos:

$$f_i(t) = K_P(w_i - w_{i,d}) + K_v(\dot{w}_i) \qquad (1)$$

where

$f_i(t)$ is the force generated by the ith actuator;

w_i, $w_{i,d}$, $\dot{w}_i$ are the length, the desired length, and velocity of the ith actuator; and

K_P, K_v are position and velocity gains.

Using this servo, a full sweep of the leg takes approximately 70 ms. This arrangement of body, leg, hip, and actuators provides a means to control the position of the foot and the hip torque needed to balance the system during locomotion.

Data from the sensors mounted on the hopping machine are digitized and transmitted to the control computer over a digital bus. These sensors include the gyroscopes, the hip-actuator potentiometers and tachometers, the leg-length potentiometer, the foot switch, and the leg-pressure sensors. These sensory data are used not only to control the machine, but also to record and analyze its behavior. The "umbilical" cable that carries the digital communication bus also carries hydraulic power for the hip actuators, compressed air that drives the hopping motion, and dc power for sensors and electronics.

To make the machine balance while traveling from place to place, the control algorithms position the foot during flight and correct the body attitude during stance. During flight the control computer chooses a forward position for the foot appropriate to the machine's rate of travel. During stance the control computer generates torques at the hip to maintain an upright body posture. The resulting control system produces running at rates of up to 2.2 m/s (4.8 mi/h), with strides of up to 0.79 m. General operation of the machine is shown in Fig. 3 by a sequence of photographs taken in one stride.
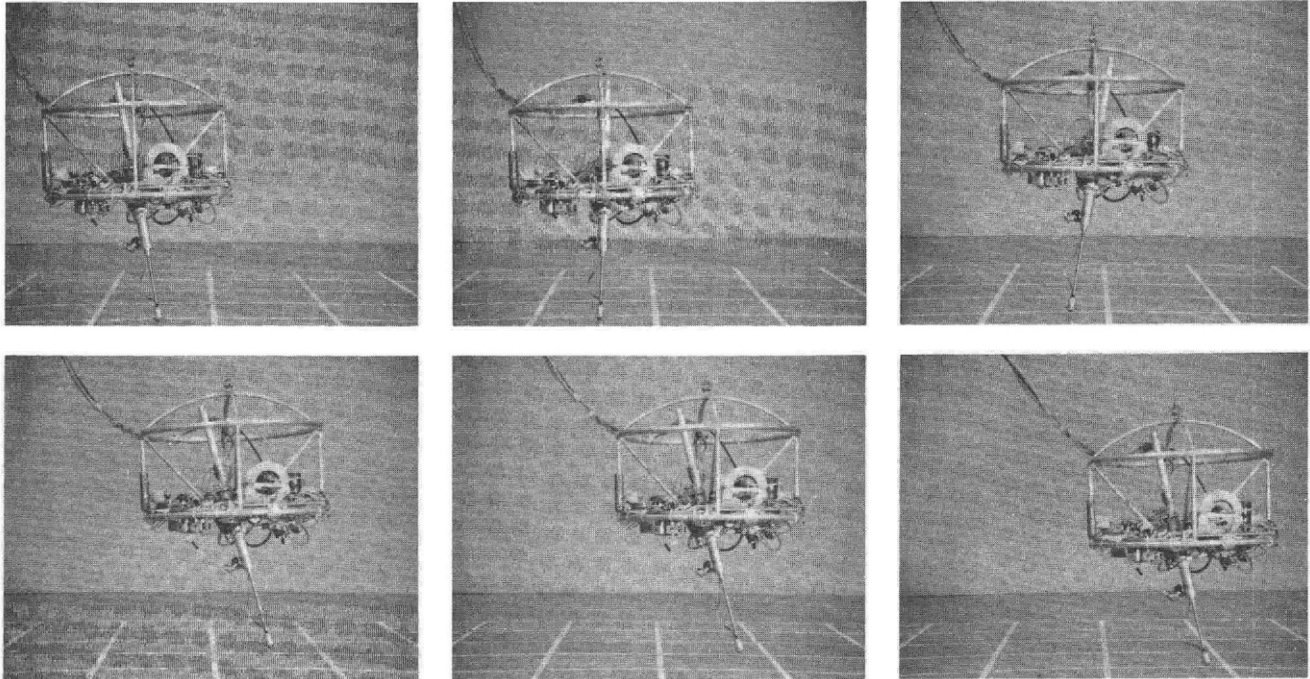
3. Control Algorithms

In this section we describe the algorithms examined for hopping and balance in the 3D machine. Since these algorithms were formulated by generalizing from the 2D machine, we also review the 2D algorithms.

Conceptually, the 2D and 3D algorithms are very similar. The basic approach is to treat the system like an inverted pendulum, and to decompose the control into independent parts. Like the 2D algorithms, the

Fig. 3. Sequence of photographs showing one complete stride of the 3D hopping machine running from left to right. Grid on floor indicates 0.5-m intervals. Running speed is about 1.75 m/s, with stride length 0.63 m and stride period 0.380 s. Adjacent frames are separated by 76 m.

3D algorithms decompose easily into three parts, one part each for control of forward running velocity, attitude of the body, and hopping height. The system controls forward running velocity by positioning the foot with respect to the projection of the center of gravity. This is done during every flight phase, when the foot is not touching the ground. The system controls the attitude of the body by torquing the hip stance when the foot is held in place by friction. The system adjusts the hopping height by regulating the amount of thrust delivered by the leg on each hop. These three parts of the control system are largely independent, with their synchronization coming from the ongoing activity of the hopping machine. It is this independence of action that makes the control system simple. The remainder of this section reviews each part of the control algorithm used in 2D and describes the corresponding extension to 3D.
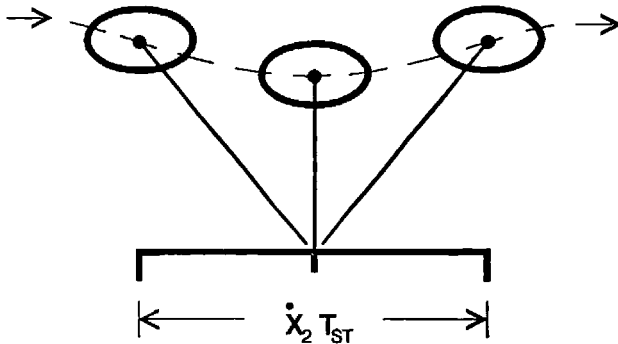
3.1. Forward Velocity

The position of the foot when it first touches the ground on each step has a powerful influence on the accelerations the system will experience during the impending support period. The algorithm that controls forward velocity must choose a position for the foot that will generate the proper accelerations. The algorithm studied here uses two factors to find a good position for the foot. One factor is the forward velocity of the system. It is used to find a nominal foot position that would generate zero net accleration during the support period. The other factor is the forward velocity error. It is used to calculate a displacement of the foot from the nominal position that will accelerate the system as required. Accelerations are required to stabilize the forward velocity against errors and to generate desired changes in running velocity. The nominal foot position and displacement of the foot combine to specify where the control system will place the foot.

The method used to find a nominal foot position that will not accelerate the system depends on producing a symmetric pattern of motion during the stance phase. During stance, when the foot is touching the ground, the one-legged system is like an inverted pendulum. An inverted pendulum may be kept from tipping over by manipulating the position of the sup-

Raibert, Brown, and Chepponis   **79**

Fig. 4. When the foot is placed in the center of the CG-print, there is a symmetric motion. The figure depicts running from left to right. The left-most drawing shows the configuration just before the foot touches the ground, the center drawing shows the configuration when the leg is maximally compressed, and the right-most drawing shows the configuration just after the foot loses contact with the ground.

Fig. 5. Behavior when the foot is displaced from the center of the CG-print. A. When the foot is placed in the center of the CG-print, the system tips neither forward nor backward, and it does not change its forward running velocity. B. When the foot is placed toward the rear of the CG-print, the body tips and accelerates forward during stance. C. When the foot is placed toward the front of the CG-print, the body tips backward and decelerates during stance. Horizontal lines indicate the CG-print for each case.
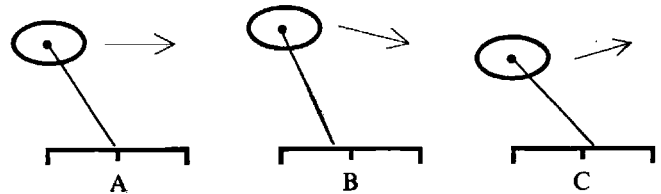
port point with respect to the center of mass in such a way that every tipping motion to one side is compensated by an equal tipping motion to the other side. For a legged system to balance, the control system can position the foot so that there are equal amounts of forward and rearward tipping, and symmetric horizontal forces acting on the ground.

Like the inverted pendulum, a legged system tips and accelerates when its point of support is not located directly below its body. The acceleration magnitude is a function of the horizontal displacement of the support point from the center of mass. A legged system will undergo no net forward acceleration during stance, when the trajectory of the foot with respect to the center of mass is symmetric about a vertical line passing through the center of mass. Figure 4 shows such a symmetric motion for a planar one-legged system. When this symmetry is achieved, the body spends about the same amount of time in front of the foot as it spends behind the foot, so the tipping moments are balanced. The horizontal components of the leg thrust, determined by the leg spring and the angle of the leg to the vertical, are balanced in a similar manner. The forward speed of the system does not change because the horizontal component of the thrust delivered by the leg to the ground averages to zero throughout the stance phase.

In order to achieve symmetry of this sort in the one-legged system, the control algorithm estimates the locus of points over which the center of gravity will travel during the next stance period. We call this locus the *CG-print;* it is analogous to a footprint. The length of the CG-print is the product of the average forward velocity and the duration of stance. The desired sym-

metry is obtained when the foot is placed in the center of the CG-print.

The control system produces accelerations by placing the foot a distance away from the center of the CG-print (Fig. 5). Placing the foot forward of the center of the CG-print causes the system to spend more time during stance with the body behind the point of support than in front of it. This creates a net backward tipping moment, a net rearward force on the body, and rearward acceleration. Placing the foot behind the center of the CG-print causes the body to spend more time in front of the point of support, creating a net forward acceleration. The algorithm implemented here uses a linear function of velocity errors to calculate displacement of the foot. It uses foot placement to generate these accelerations when the forward velocity deviates from its desired value or when there is a need to change running speed.

The equations that were used to control forward velocity for the 2D case are given in terms of the variables defined in Fig. 6. First, the algorithm calculates a desired foot position as a function of the forward velocity and the velocity error:

$$x_{F,d} = \frac{\dot{x} T_{ST}}{2} + K(\dot{x} - \dot{x}_d), \qquad (2)$$

where

$x_{F,d}$ is the desired forward position for the foot;
$\dot{x}, \dot{x}_d$ are the forward and desired forward velocity; and
T_{ST} is the duration of stance.

Once the desired displacement for the foot is known, the algorithm determines the hip angle that will place the foot there:

Fig. 6. Diagram of planar one-legged system that shows variables used in calculating placement of the foot to control forward running velocity.
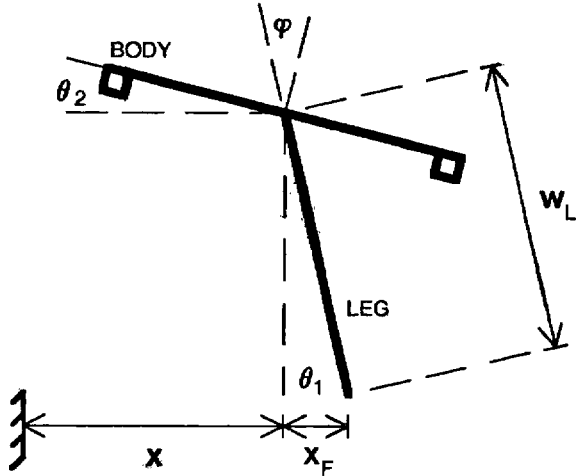
$$\psi_d = F(x_{F,D}) = \theta_2 + \text{Arcsin}\left[\frac{x_{F,d}}{w_L}\right]. \qquad (3)$$

To generalize these equations for the 3D case, we modify the forward velocity to include an additional direction of travel. Now the forward velocity has two components, either an x and y component, as used here, or a magnitude and direction. The kinematics that transform desired foot position into hip angles must also be changed, since body orientation will have three rotations for the 3D case. Since the forward velocity will now have two components to control, we replace each position and velocity in (Eq. 2) with a vector:

$$\mathbf{X}_{F,d} = \frac{\dot{\mathbf{X}}T_{ST}}{2} + K(\dot{\mathbf{X}} - \dot{\mathbf{X}}_d), \qquad (4)$$

where

$\mathbf{X}_{F,d} = [x_{F,d}, y_{F,d}]^T$ and
$\dot{\mathbf{X}} = [\dot{x}, \dot{y}]^T$.

The forward velocity, $\dot{\mathbf{X}}$, desired forward velocity, $\dot{\mathbf{X}}_d$, and desired position of the foot with respect to the hip, $\mathbf{X}_{F,d}$, are expressed in coordinate systems that do not change orientation in space. Therefore, the desired motion of the system and measurements of its behavior are expressed in terms of nonrotating coordinates. In practive they are aligned with the walls of our laboratory.

Once the desired position of the foot with respect to

the hip is known from (Eq. 4), we find the actuator lengths that will correctly position the foot:

$$\mathbf{W}_d = \mathbf{F}(\mathbf{X}_{F,d}), \qquad (5)$$

where $\mathbf{W}_d = [w_1, w_2]^T$, a vector of desired hip-actuator lengths.

$\mathbf{F}$ is a function that expresses the kinematic relationship between hip-actuator lengths and foot position. It is an implicit function of leg length, w_L, and the orientation of the body in space, Θ. $\mathbf{F}$ and its inverse, $\mathbf{F}^{-1}$, are given in Appendix B. Once $\mathbf{W}_d$ is known, the linear servo (Eq. 1) positions the foot.

Equations (4 and 5) can be used to control forward velocity once values for the forward velocity, $\mathbf{X}$, desired forward velocity, $\dot{\mathbf{X}}_d$, and the duration of stance, T_{ST}, are known. The foot does not move with respect to the ground during stance, so the forward velocity is the negative of the velocity of the foot with respect to the hip:

$$\dot{\mathbf{X}} = -\dot{\mathbf{X}}_F. \qquad (6)$$

The position of the foot with respect to the hip is given by:

$$\mathbf{X}_F = \mathbf{F}^{-1}(\mathbf{W}). \qquad (7)$$

Measurements of $\mathbf{W}$, w_L, and Θ are available from the actuator sensors and the gyroscopes. We estimate the velocity during stance by numerically differentiating $\mathbf{X}_F$ as determined from (Eq. 7). We assume that the forward velocity does not change appreciably during flight. Since the duration of stance, T_{ST}, is governed by the springiness of the leg, it is largely independent of hopping height and nearly constant for a given leg stiffness. The control system uses the measured duration of the last stance phase as the expected duration of the next stance phase. The desired forward velocity, $\dot{\mathbf{X}}_d$, is obtained from either a two-axis joystick that is manipulated by an operator, or a test program that generates programmable velocity trajectories.

In the current implementation, the center of the CG-print is estimated as $\dot{\mathbf{X}}T_{ST}/2$. This estimate is not very good at high velocity or when the duration of stance is very long. When running at high velocity, horizontal forces generated by the leg decelerate the system substantially during the first half of stance,

Raibert, Brown, and Chepponis   **81**

then accelerate it again during the second half of stance. The average forward velocity during stance is less than the forward velocity when the foot first touches the ground or when it leaves the ground. Therefore, the length of the CG-print is substantially shorter than estimated. While we are working on better methods for estimating the CG-print (Raibert et al. 1983), this problem is not too important in practice. The estimation error results in a velocity-dependent, steady-state error in forward velocity that increases at high rates of travel.

3.2 BODY ATTITUDE

Since angular momentum of legged systems is conserved during flight, a control system can manipulate the body attitude only during stance, when there is traction between the foot and the ground. Torques generated between the leg and the body during stance are used to servo the attitude of the body to a desired orientation. For the planar case the stance servo was

$$\tau(t) = K_P(\theta_2 - \theta_{2,d}) + K_V(\dot{\theta}_2), \tag{8}$$

where

τ is the hip torque;
K_P, K_V are position and velocity gains; and
$\theta_{2,d}$ is the desired attitude of the body.

For the 3D system, both the pitch and roll axes must be controlled during stance:

$$\begin{aligned} f_1 &= K_P(\theta_P - \theta_{P,d}) + K_V(\dot{\theta}_P), \\ f_2 &= K_P(\theta_R - \theta_{R,d}) + K_V(\dot{\theta}_R), \end{aligned} \tag{9}$$

where

f_1, f_2 are the hip-actuator forces;
K_P, K_V are position and velocity feedback gains; and
$\theta_{P,d}$, $\theta_{R,d}$ are the desired pitch and roll angles, zero in this paper.

The pitch and roll angles upon which these attitude-control servos operate are defined in a coordinate system that moves and rotates with the body. They are not corrected for rotations of the body about its yaw axis, as the forward position and velocities are. The gyroscope is aligned so that the signal from one axis

can be used to servo one hip actuator, and the signal from the other axis can be used to servo the other hip actuator. This simple arrangement requires very little computation and provides very good stability.

In addition to keeping the body erect, the control system is responsible for controlling the facing direction of the body, the yaw angle. This is a degree of freedom that has no counterpart in 2D. In principle, it is possible to generate torques about the yaw axis for this purpose, despite the lack of an actuator that twists the foot about the leg axis. When the control system places the foot to one side of the direction of travel and torques fore or aft at the hip during stance, a moment is developed about the yaw axis of the system. In order to stabilize the system during such a maneuver, the foot can be offset in one direction on one hop, and in the other direction on the next hop.

We have found through experimentation and subsequent analysis that the maximum yaw torque that can be generated in this manner is substantially smaller than the disturbance torque generated by the umbilical cable that connects the machine to power supplies and computer. Therefore, the control system was not able to generate adequate yaw torque to control the facing direction of the 3D hopping machine. Instead, the control system used measurements of the yaw angle to compensate for the facing direction of the machine, without trying to control it.

3.3. HOPPING HEIGHT

For a legged system to locomote, each leg must alternate between a support phase, in which the foot touches the ground and bears weight, and a transfer phase, in which the foot is elevated to move from one foothold to another. Such alternation between loaded and unloaded phases underlies the normal activity of all sorts of legs in all sorts of legged systems. For a system with one leg, this alternation is the hopping cycle.

Unlike control of forward velocity and body attitude, control hopping height is no different in 3D than it was in 2D. Hopping is accomplished by exciting the resonant spring-mass system formed by the leg and body. In principle, the height of each hop will be determined by the kinetic and potential energies of the system, and the loss encountered on each bounce. Manipulation of these energies could be used to con-

trol the height to which the system hops (Raibert, 1984). A simpler technique was used in practice.

If the system were left to bounce passively on the springy leg, losses in the sliding friction of the air cylinder and in accelerating and decelerating the unsprung mass of the leg would soon cause the machine to come to rest. Measurements of the decay in hopping height during passive bouncing showed that such energy losses amounted to about a 35% loss on each bounce. The leg actuator delivers a vertical thrust on each cycle that just compensates for these losses.

Hopping height is regulated by providing a fixed thrust on each hop. Equilibrium occurs when the energy lost in one hopping cycle equals the energy introduced through the leg actuator. Since losses are monotonic with hopping height, a unique hopping height exists for each value of leg-actuator thrust. Details of the relationship between hopping height and duration of thrust can be determined empirically.

4. Experimental Results

The one-legged machine described in Section 2 was used to evaluate and refine the control algorithms and to demonstrate balance in a 3D running machine. The height, velocity, and attitude-control algorithms of the last section were implemented in a set of control programs that ran on a control computer. These programs controlled the machine and recorded its behavior. The experiments tested velocity control, position control, the ability to follow a simple path, and the hopping machine's resistance to disturbances.

We examined the system's ability to regulate forward running velocity by having the control computer specify a ramp in desired velocity. The results are plotted in Fig. 7. These data show the machine, first hopping in place, then running at increasing rates up to about 1.7 m/s. Throughout the run, velocity was controlled to within about 0.2 m/s of the desired value. This accuracy is typical. When the desired velocity was set to zero at $t = 5.3$ s, it took about 0.5 s for the velocity to change. This was the delay between the change in $\dot{x}_d$ and the following touchdown.

During running, the leg and body counter-oscillate, as shown in the plots of X_F, θp and θR in Fig. 7C and D. The back-and-forth motions of the leg were not explicitly programmed but resulted from interactions

between the velocity controller, which positioned the leg forward during flight, and the attitude controller, which operated during stance. Oscillations of the body were expected, because angular momentum is conserved during flight and attitude correction occurs only during stance. Asymmetric oscillation of body attitude was also expected, since the desired body angle, Θ_d, was always zero. The relative magnitudes of the pitch and roll oscillations varied as the facing direction of the machine, its yaw angle, changed.

In another experiment, the desired speed was held constant, but the desired direction was changed abruptly by 90°. The results are shown in Fig. 8. It took two hops for the system to change direction, but speed was erratic after the turn.

A position-control algorithm was used to make the hopping machine hop in one place and to translate from place to place. The position-control algorithm transforms position errors into desired velocities:

$$\dot{X}'_d = K_P(X - X_d) + K_V \dot{X},$$
$$\dot{X}_d = \min\{\dot{X}'_d, \dot{X}_{d,\max}\}, \tag{10}$$

where

K_P, K_V are diagonal position and velocity gain matrices; and

$\dot{X}_{d,\max}$ is a limit on the allowable velocity.

The control programs obtained information about the machine's position in the room in two ways. They could estimate the position of the machine by numerically integrating the forward velocity estimate, $\dot{X}$. Position information was also available from an electro-optical sensor (Selspot) mounted on the ceiling of the laboratory. Data could be read from this sensor by the control computer one time per hop in order to calculate a new desired velocity using (Eq. 10). One may think of the ceiling-mounted sensor as serving the same role as the geosynchronous satellites used for global navigation. Our geosynchronous satellite had a very low orbit.

Figure 9 is a plot of the machine's position as it hopped in place, using the integrator position values for control. The machine stayed within 0.25 m of the setpoint. Deviations of this magnitude were typical for stationary hopping. In addition to integrator data, data are plotted from the electro-optical measurement. The deviations in these curves shows that the integrator
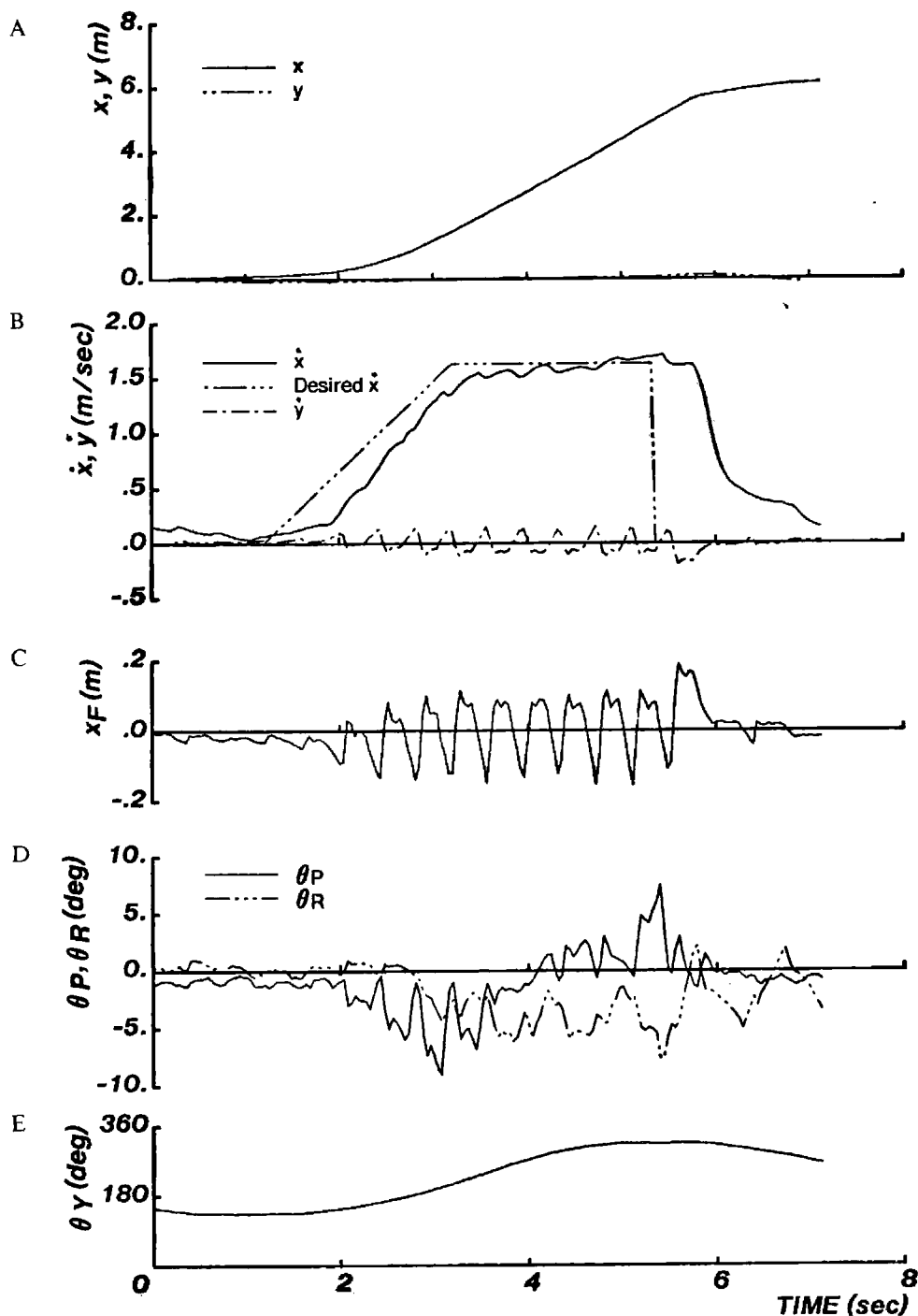
83

Fig. 8. A step change in desired direction was programmed to generate a right-angle turn, while holding desired speed constant. The top two curves (A and B) plot the x and y velocities, and the bottom two (C and D) show the speed and heading. The turn was completed in two steps.
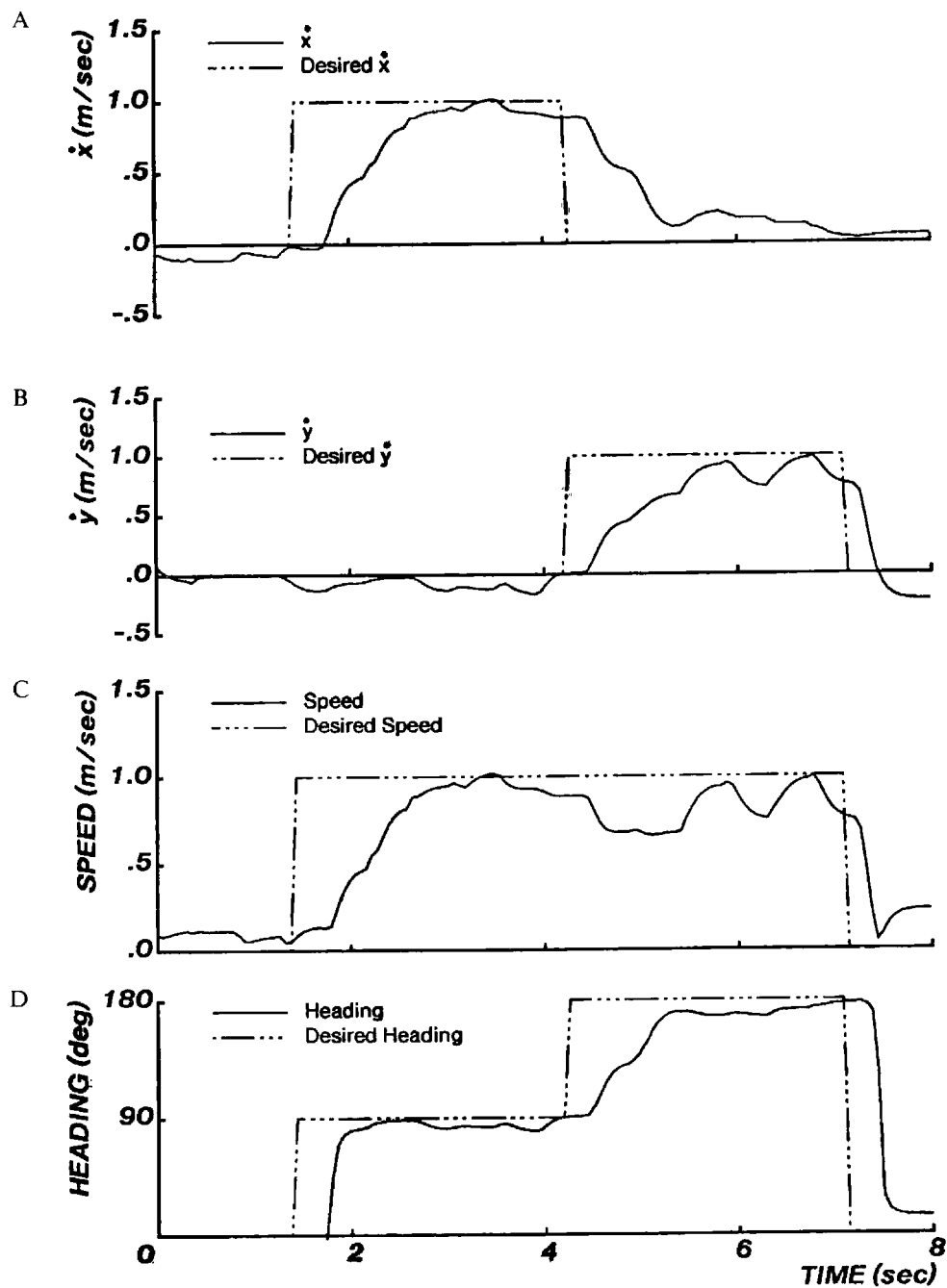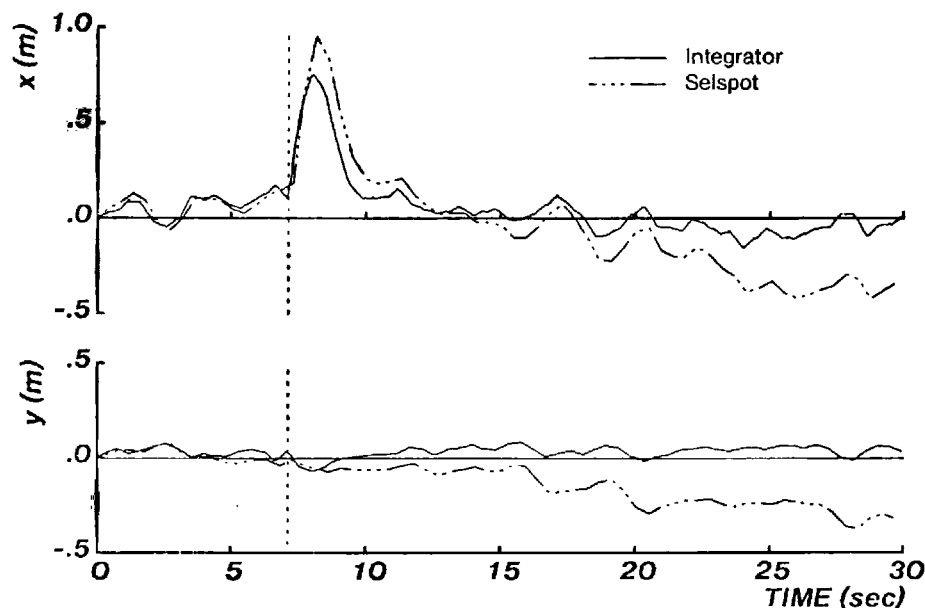
drifts by about 0.005 m per hop. This means that if the machine were instructed to hop in one spot, it might drift 1 m in 1 min. Informal experiments with blind-folded humans hopping on one leg indicate that they drift by similar amounts. In the case of the hopping machine, the primary sources of drift were gyroscope calibration errors and unwanted forces exerted on the machine by the umbilical cable.

Figure 9 also shows the response to an external disturbance. After about 7 s, the experimenter delivered a sharp horizontal jab to the body as the machine hopped in place (see dotted vertical line in Fig. 9.) The machine maintained its balance and returned to the position setpoint after a few seconds. The control system tolerated fairly strong disturbances of this sort. The system also tolerated substantial torsional disturbances of this sort, as well as moderate roll and pitch disturbances.

In order to measure performance under position control, the control computer specified desired positions according to a preplanned sequence. An operator pressed a button every time he wanted the next position setpoint from the sequence. In this way, we programmed a square path, 2 m on a side. Figure 10 plots data obtained while traversing such a path, and Fig. 11 is a photograph of the machine traversing a square path. The data shown in Fig. 10 are pretty good, with

the exception of a fixed position error of about 0.3 m when $y_d = 0$. This error was caused by the umbilical cable, which was just long enough to permit the machine to reach $y = 0$. The system came to equilibrium where the force exerted by the umbilical cable equaled the accelerations produced by the control system.

5. Discussion

The 3D control system reported in this paper is very much like two separate 2D control systems operating at right angles to one another. If we write (Eqs. 4 and 5) in terms of the components of **X**, then we get two sets of equations that are each like the 2D velocity-control equation, (Eq. 2).

Another way to view the system is as an implementation of the plane-of-motion idea described by Murthy and Raibert (1983). They proposed that locomotion in 3D might be best understood by thinking in terms of decomposition into a planar part and an extraplanar part. The planar part of the control was just like the system used for a 2D one-legged system. The extraplanar part was responsible for maintaining the planarity of motion so that the planar part could operate effectively. The control algorithms described in this paper are perfectly consistent with this plane-of-

between representing a point in Cartesian coordinates and in polar coordinates.

For the experiments reported in this paper, $\theta_{P,D} = \theta_{R,D} = \dot{\theta}_{P,D} = \dot{\theta}_{R,D} = 0$. As a result, the algorithm that controlled attitude of the body, (Eq. 9), produced an asymmetric oscillation of θ_P and θ_R. The body was made erect at lift-off, but because angular momentum must be conserved during flight, motion of the leg caused motion of the body. Furthermore, at the beginning of stance, the body was suddenly made erect. It should be possible to reduce the asymmetry of θ_P and θ_R oscillations, and to eliminate the sudden erection of the body at touchdown, by choosing the roll and pitch setpoints to satisfy

$$J_{\text{BODY}}\theta_P + J_{\text{LEG}}\phi_P = 0, \quad J_{\text{BODY}}\dot{\theta}_P + J_{\text{LEG}}\dot{\theta}_P = 0,$$
$$J_{\text{BODY}}\theta_R + J_{\text{LEG}}\phi_R = 0, \quad J_{\text{BODY}}\dot{\theta}_R + J_{\text{LEG}}\dot{\theta}_R = 0, \quad (11)$$

where

J_{BODY} is the moment of inertia of the body about the hip;
J_{LEG} is the average moment of inertia of the leg about the hip;
θ_P, θ_R are the pitch and roll angles of the body; and
ϕ_P, ϕ_R are the pitch and roll angles of the leg.

These equations specify that the attitude of the leg and body remain vertical, and that the average angular rate of the system remain zero. We have not yet tested this approach extensively.

In the last section we reported a failure to control the facing direction of the machine. The sources of yaw torque available in the machine we built were inadequate to overcome the disturbance torque generated by the umbilical cable. As a practical problem, this failure did not interfere with the experiments, but was finessed with a little extra computing. Moreover, yaw control is not likely to be a difficult problem for legged vehicles. Useful legged vehicles will not have umbilical cables, and their legs can be designed to generate yaw torques directly if required. For systems with more than one leg, legs can act together to generate substantial yaw torque.

The decision to explore locomotion in a system with just one leg was motivated by our desire to focus on balance as the primary research issue. A one-legged system must balance in order to remain upright during locomotion, it must have a ballistic phase on each

motion approach. During each flight period, the control system uses the instantaneous forward velocity to determine the plane of motion and chooses a foot position with respect to this plane. The position of the foot within the plane will determine the forward acceleration, while the position of the foot perpendicular to the plane of motion will determine the change in orientation of the plane of motion on the next step.

Both of these conceptualizations are correct and consistent. Both explanations can be summarized as follows. For every forward velocity there is a position for the foot that will provide no net acceleration during stance — the forward velocity when the foot leaves the ground will be the same as the forward velocity when the foot last touched the ground. This position is a velocity-fix point. The displacement of the foot from this position determines the acceleration of the system and therefore the change of speed and direction. The position that generates zero net acceleration is approximated equally well by the pair of perpendicular CG-prints and by the single CG-print in the plane of motion. The difference is analogous to the difference

step, and it can move with substantial velocity. These characteristics are not found in most previous walking machines, which are statically stable. It was also our goal to avoid the difficult problem of coordinating many legs until we had more experience with one.

While the primary purpose of using a one-legged machine for these experiments was to focus on balance, an additional goal was to develop a model that could explain the behavior of more complicated systems that run. If we ignore the third dimension, generalizing from the one-legged machine to the two-legged hopping kangaroo is very easy. A direct comparison can be made between the motions of the hopping machine's one leg and the motions of the kangaroo's pair of legs. The primary difference is that the kangaroo uses its tail to help compensate for the large sweeping motions of the legs, so that the body need not react by pitching so much on each hop. The control system could still regulate hopping height, body attitude, and velocity, as before.

Many characteristics of the running biped are also similar to a system that runs on one leg, including the alternation between stance and flight, the regular vertical oscillations, and the periods of one-legged support. In the case of the biped, the two legs swing in opposite directions, making pitching motions of the body and a tail unnecessary. Think of a biped as a hopping machine that substitutes a different leg on each stride. The same algorithms that were used to control the three-dimensional hopping machine could be used without modification to control a biped. Extensions of this approach to systems with more legs is under way. Preliminary results are reported by Murphy and Raibert (1984).

6. Summary

This paper presents a set of algorithms for control of a machine that runs and balances on one leg in 3D, and it describes experiments that evaluate their performance. The goal was to explore the fundamental problems of active balance in dynamic legged systems.

We found that the algorithms designed for control of a planar one-legged system generalized to 3D with surprising ease. As in 2D, the control problem decomposed into three separate parts, each synchronized by the ongoing behavior of the machine. One control part

regulates the forward running velocity of the system and the rate of turn by placing the foot a specific distance in front of and to the side of the hip as the hopping machine approaches the ground on each step. The second control part maintains the body in an erect posture by servoing the hip during stance. The third control part determines hopping height by choosing a fixed amount of energy to inject on each hopping cycle. The control algorithms are very simple because these three functions are treated independently.

Experiments showed that the 3D hopping machine balanced without external support, while hopping in place and while traveling about the laboratory. It tracked a velocity ramp and sudden changes in desired direction with 0.25-m/s accuracy. At higher speeds the system consistently ran slower than specified due to inaccuracies in estimating the CG-print. Maximum recorded speed was 2.2 m/s (4.8 mi/h). In position control the system determined the position of the machine in the laboratory by integrating the estimated running velocity. With a stationary position setpoint, the machine could hop in place with about ± 0.25-m accuracy. The machine also traversed a square path, but the path accuracy suffered due to interference from forces generated by the umbilical cable. The system continued to balance while the experimenter delivered a sudden jab to the machine's body with his hand.

While legged vehicles with just one leg could very well turn out to have utility in their own right, the real purpose of these experiments was to explore the fundamental principles of balance in a simple legged system. A system with just one leg was a good choice for these experiments because balance is of paramount importance to its locomotion, and because the problem of coordinating many legs was avoided. The results of this work may help us to understand better both the overall behavior of legged systems that actively balance and the individual behavior of each leg in systems with more than one.

7. Acknowledgments

Appendix A: Physical Parameters of the 3D One-Legged Machine

Parameter	Metric Units	English Units
Overall height	1.10 m	43.5 in
Overall width	0.76 m	30.0 in
Hip height	0.58 m	23.0 in
Total mass (body and leg)	17 kg	38 lbm
Unsprung leg mass	0.91 kg	2.0 lbm
Ratio: body mass to unsprung leg mass	18/1	18/1
Body moment of inertia	0.709 kg/m²	2420 lbm/in²
Leg moment of inertia	0.111 kg/m²	380 lbm/in²
Ratio: body moment of inertia to leg moment of inertia	6.4/1	6.4/1
Leg Vertical Motion		
Stroke	0.25 m	10.0 in
Ideal no-load stroke time	0.031 s at 620 kPa*	0.031 s at 90 psi gauge
Static force	630 N at 620 kPa	140 lb at 90 psi gauge
Ratio: static force to weight	3.7/1	3.7/1
Theoretical maximum work per stroke	160 N·m	1400 lbin
Leg Sweep Motion		
Sweep angle	1.00 rad/0.71 rad	57°/41°
Ideal no-load sweep time	0.069 s at 14 MPa†	0.069 s at 2,000 psi
Static torque	90 N·m at 14 MPa	800 lbin/1,200 lbin at 2,000 psi
Theoretical maximum work per stroke	83 N·m	740 lbin

* Kilo Pascal.

† Mega Pascal.

Appendix B: Kinematics of the 3D Machine

We define three coordinate frames $\{W\}$, $\{H\}$, and $\{B\}$. Frame $\{W\}$ is the base coordinate frame, which is fixed in the laboratory. The origin of frame $\{H\}$ moves with the hip, but its orientation remains parallel to $\{W\}$. Think of frame $\{H\}$ as attached to the innermost gimbal of the gyroscope. For $\{W\}$ and $\{H\}$, z is aligned with the gravity vector, and positive upward. Frame $\{B\}$ is fixed to the body. Its origin also moves with the hip, but $\{B\}$ changes orientation with respect to $\{W\}$ and $\{H\}$. The Euler angles that specify the orientation of $\{B\}$ are $(\theta_Y, \theta_R, \theta_P)$. The hip and leg actuators determine the position of the foot in frame $\{B\}$.
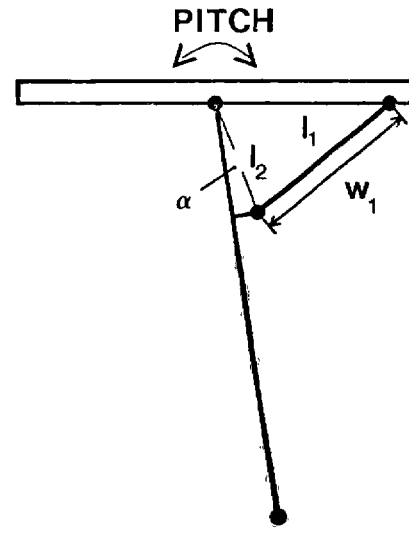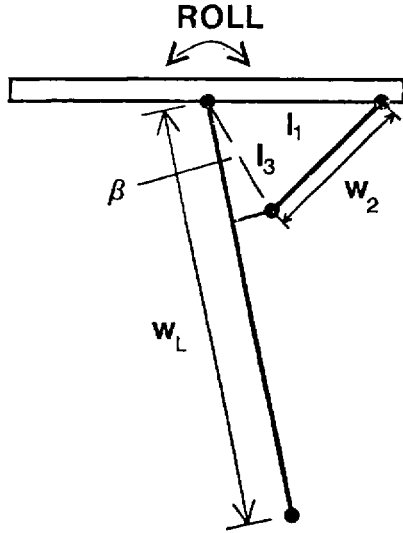
Let the vector $^P X$ be a vector $[x, y, z, 1]^T$ expressed in coordinate frame $\{P\}$. The transformation from coordinate frame $\{B\}$ to $\{H\}$ is

$$^H X = {}_B^H T {}^B X \tag{12}$$

$${}_B^H T =$$

$$\begin{bmatrix} \cos(\theta_P)\cos(\theta_Y) - \sin(\theta_P)\sin(\theta_R)\sin(\theta_Y) & -\cos(\theta_R)\sin(\theta_Y) \\ \cos(\theta_P)\sin(\theta_Y) + \cos(\theta_Y)\sin(\theta_P)\sin(\theta_R) & \cos(\theta_R)\cos(\theta_Y) \\ \cos(\theta_R)\sin(\theta_P) & -\sin(\theta_R) \\ 0 & 0 \end{bmatrix}$$

$$\begin{bmatrix} -\cos(\theta_P)\sin(\theta_R)\sin(\theta_Y) - \cos(\theta_Y)\sin(\theta_P) & 0 \\ \cos(\theta_P)\cos(\theta_Y)\sin(\theta_R) - \sin(\theta_P)\sin(\theta_Y) & 0 \\ \cos(\theta_P)\cos(\theta_R) & 0 \\ 0 & 1 \end{bmatrix}$$

Transformation from frame $\{H\}$ to $\{B\}$ is

Fig. 12. Kinematics of actuators, hip, and leg. Actuator lengths are represented by w_1 and w_2, and leg length by w_L. $l_1 = 0.345$ m,
$l_2 = 0.0508$ m, $l_3 = 0.0762$m,
$\alpha = 8.46°$, $\beta = 27.28°$.

ROLL

PITCH

$$^\mathbf{B}\mathbf{X} = {}^\mathbf{B}_\mathbf{H}\mathbf{T}\,{}^\mathbf{H}\mathbf{X} \tag{13}$$

$$^\mathbf{B}_\mathbf{H}\mathbf{T} =$$

$$\begin{bmatrix} \cos{(\theta_P)}\cos{(\theta_Y)} - \sin{(\theta_P)}\sin{(\theta_R)}\sin{(\theta_Y)} \\ -\cos{(\theta_R)}\sin{(\theta_Y)} \\ -\cos{(\theta_P)}\sin{(\theta_R)}\sin{(\theta_Y)} - \cos{(\theta_Y)}\sin{(\theta_P)} \\ 0 \end{bmatrix}$$

$$\begin{matrix} \cos{(\theta_P)}\sin{(\theta_Y)} + \cos{(\theta_Y)}\sin{(\theta_P)}\sin{(\theta_R)} & \cos{(\theta_R)}\sin{(\theta_P)} & 0 \\ \cos{(\theta_R)}\cos{(\theta_Y)} & -\sin{(\theta_R)} & 0 \\ \cos{(\theta_P)}\cos{(\theta_Y)}\sin{(\theta_R)} - \sin{(\theta_P)}\sin{(\theta_Y)} & \cos{(\theta_P)}\cos{(\theta_R)} & 0 \\ 0 & 0 & 1 \end{matrix}$$

Relationships between actuator lengths and position of foot with respect to the body in frame {**B**} are shown in (Fig. 12). First the forward solution:

$$^\mathbf{B}\mathbf{X}_\mathbf{F} = {}^\mathbf{B}_\mathbf{A}\mathbf{T}(\mathbf{W}) \tag{14}$$

$$^\mathbf{B}_\mathbf{A}\mathbf{T}(\mathbf{W}) =$$

$$x = w_L \cos\left\{ \mathrm{Arccos}\left[\frac{w_1^2 - l_1^2 - l_2^2}{-2l_1 l_2} \right] + \alpha \right\}$$

$$y = w_L \cos\left\{ \mathrm{Arccos}\left[\frac{w_2^2 - l_1^2 - l_3^2}{-2l_1 l_3} \right] + \beta \right\}$$

$$z = \sqrt{w_L^2 - x^2 - y^2}$$

$$^\mathbf{B}\mathbf{X}_\mathbf{F} = [x, y, z, +1]^T.$$

The inverse solution is

$$\mathbf{W} = {}^\mathbf{B}_\mathbf{A}\mathbf{T}(^\mathbf{B}\mathbf{X}_\mathbf{F}) \tag{15}$$

$$\mathbf{W} = [w_1, w_2, w_L]^T$$

$$w_1 = \sqrt{ l_1^2 + l_2^2 - 2l_1 l_2 \cos\left\{ \mathrm{Arccos}\left[\frac{x}{-w_L} \right] - \alpha \right\} }$$

$$w_1 = \sqrt{ l_1^2 + l_3^2 - 2l_1 l_3 \cos\left\{ \mathrm{Arccos}\left[\frac{y}{-w_L} \right] - \beta \right\} }$$

$$w_L = -\sqrt{x^2 + y^2 + z^2}.$$

The overall transformations between actuator variables and foot position in {**H**} are

$$^\mathbf{H}\mathbf{X}_\mathbf{F} = {}^\mathbf{H}_\mathbf{B}\mathbf{T}\,{}^\mathbf{B}_\mathbf{A}\mathbf{T}(\mathbf{W}) = \mathbf{F}^{-1}(\mathbf{W}), \tag{16}$$

$$\mathbf{W} = {}^\mathbf{A}_\mathbf{B}\mathbf{T}(^\mathbf{B}_\mathbf{H}\mathbf{T}\,{}^\mathbf{H}\mathbf{X}_\mathbf{F}) = \mathbf{F}(^\mathbf{H}\mathbf{X}_\mathbf{F}). \tag{17}$$

REFERENCES

Beletskii, V. V., and Kirsanova, T. S. 1976. Plane linear models of biped locomotion. *Izv. An SSSR. Mekhanika Tverdogo Tela* 11(4):51–62.

Bessanov, A. P., and Umnov, N. V. 1973 (Udine, Italy). The analysis of gaits in six-legged vehicles according to their static stability. *Proc. Symp. Theory and Practice Robots and Manipulators.* Amsterdam: Elsevier.

Ceranowicz, A. Z. 1979. Planar biped dynamics and control.

Ph.D. thesis, The Ohio State University Department of Electrical Engineering.

Frank, A. A. 1968. Automatic control systems for legged locomotion machines. Ph.D. thesis, University of Southern California.

Frank, A. A. 1970. An approach to the dynamic analysis and synthesis of biped locomotion machines. *Med. Biol. Eng.* 9:465–476.

Golliday, C. L., Jr., and Hemami, H. 1977. An approach to analyzing biped locomotion dynamics and designing robot locomotion controls. *IEEE Trans. Automatic Contr.* AC-22 (6):963–972.

Gubina, F. 1972. Stability and dynamic control of certain types of biped locomotion. Paper delivered at IV Symp. External Contr. Human Extremities, Dubrov.

Hemami, H. 1980. A feedback on-off model of biped dynamics. *IEEE Trans. Syst. Man Cybern.* SMC-10 (7):376–383.

Hemami, H., and Farnsworth, R. L. 1977. Postural and gait stability of a planar five link biped by simulation. *IEEE Trans. Automatic Contr.* AC-22 (3):452–458.

Hemami, H., and Golliday, C. L., Jr. 1977. The inverted pendulum and biped stability. *Math. Biosci.* 34:95–110.

Higdon, D. T., and Canon, R. H., Jr. 1963. On the control of unstable multiple-output mechanical systems. *Proc. Winter Annual Meeting.* New York: American Society of Mechanical Engineers.

Hirose, S., and Umetani, Y. 1980 (Sept. 18–Oct. 1). The basic motion regulation system for a quadruped walking vehicle. Paper delivered at the ASME Conf. Mechanisms, Los Angeles.

Kato, T., et al. 1981 (Sept. 8–12). The realization of the quasi-dynamic walking by the biped walking machine. Paper delivered at the 4th Symp. Theory and Practice of Robots and Manipulators.

Manter, J. 1938. Dynamics of quadrupedal walking. *J. Exp. Biol.* 15(4):522–539.

Matsuoka, K. 1979. A model of repetitive hopping movements in man. Paper delivered at Fifth World Congress Theory of Machines and Mechanisms.

Matsuoka, K. 1980. A mechanical model of repetitive hopping movements. *Biomechan.* 5:251–258 (in Japanese).

McGhee, R. B., and Buckett, J. R. 1977. Hexapod. *Interface Age* 2(7):25–29.

McGhee, R. B., and Kuhner, M. B. 1969. On the dynamic stability of legged locomotion systems. *Advances in external control of human extremities,* ed. M. M. Gavrilovic and A. B. Wilson, Jr. Belgrade.

Miura, H., and Shimoyama, I. 1980. Computer control of an unstable mechanism. J. Fac. Eng. 17:12–13 (in Japanese).

Murphy, K., and Raibert, M. H. 1984. Trotting and bounding in a planar two-legged model. *Proc. Theory and Practice Robots and Manipulators.* Amsterdam: Elsevier.

Murthy, S. S., and Raibert, M. H. 1983 (Apr. 4–6, Toronto). 3D balance in legged locomotion: modeling and simulation for the one-legged case. Paper delivered at ACM Inter-Disciplinary Workshop on Motion: Representation and Perception.

Raibert, M. H. 1984. Hopping in legged systems—modeling and simulation for the 2D one-legged case. *IEEE Trans. Syst. Man Cybern.* 14(3).

Raibert, M. H., and Brown, H. B., Jr. 1984. Experiments in balance with a 2D one-legged hopping machine. *ASME J. Dyn. Syst. Measurement Contr.* 106(2).

Raibert, M. H., and Sutherland, I. E. 1983. Machines that walk. *Scientific American* 248(1):44–53.

Raibert, M. H., and Wimberly, F. C. 1984. Tabular control of balance in a dynamic legged system. *IEEE Trans. Syst. Man Cybern.* 14(3).

Raibert, M. H., et al. Dynamically stable legged locomotion—third annual report. Tech. Rept. CMU-RI-TR-83. Pittsburgh: Carnegie-Mellon University, Robotics Institute.

Seifert, H. S. 1967. The lunar pogo stick. *J. Spacecraft Rockets* 4(7):941–943.

Sutherland, I. E., 1983. *A walking robot.* Pittsburgh: Marcian Chronicles.

Vukobratović, M. 1973 (Udine, Italy). Dynamics and control of anthropomorphic active mechanisms. *Proc. 1st Symp. Theory and Practice Robots and Manipulator Systems.* Amsterdam: Elsevier,

Vukobratović, M., and Okhotsimskii, D. E. 1975. Control of legged locomotion robots. Paper delivered at Fed. Automatic Contr., Plenary Session.

Vukobratović, M., and Stepaneko, Y. 1973. Mathematical models of general anthropomorphic systems. *Math. Biosci.* 17:191–242.